Instantaneous Normal Mode Analysis of Melting of Finite Dust Clusters

André Melzer and André Schella
Institut für Physik, Ernst-Moritz-Arndt-Universität Greifswald, 17489 Greifswald, Germany

Jan Schablinski, Dietmar Block, and Alexander Piel
Institut für Experimentelle und Angewandte Physik, Christian-Albrechts-Universität zu Kiel, 24098 Kiel, Germany

(Received 9 February 2012; published 29 May 2012)

The experimental melting transition of finite two-dimensional dust clusters in a dusty plasma is analyzed using the method of instantaneous normal modes. In the experiment, dust clusters are heated in a thermodynamic equilibrium from a solid to a liquid state using a four-axis laser manipulation system. The fluid properties of the dust cluster, such as the diffusion constant, are measured from the instantaneous normal mode analysis. Thereby, the phase transition of these finite clusters is approached from the liquid phase. From the diffusion constants, unique melting temperatures have been assigned to dust clusters of various sizes that very well reflect their dynamical stability properties.

DOI: 10.1103/PhysRevLett.108.225001 PACS numbers: 52.27.Lw, 64.60.an

Phase transitions in finite systems (''clusters'') generally differ from those of bulk matter. Nevertheless, solid and liquid ''phases'' in finite systems can be successfully identified analogously to bulk matter [1]. Hence, the understanding of melting transitions in such finite clusters allows an insight into bulk phase transitions or the behavior of finite systems in general. A paradigm for finite systems are clusters of trapped charged particles, such as ions in traps [2], electrons on liquid helium [3], electrons in quantum dots [4], or charged microspheres in a plasma discharge: so-called dust clusters [5–8].

The thermodynamic quantities of finite clusters (e.g., specific heat) do not show sharp transitions [9], which makes it difficult to distinguish a solid from a liquid phase. However, upon heating, Lindemann-like fluctuations of the particles around their equilibrium position start to grow [10–15] until the ordered arrangement of particles in the cluster is lost. In finite two-dimensional (2D) systems, the loss of order occurs in two steps starting with a loss of orientational correlation and followed by a loss of radial correlation. Attempts have been made to assign criteria for the melting point from the particle configurations and their fluctuations [10,16]. In all these approaches, the phase transition is assigned to a loss of structural properties of an ordered particle arrangement.

In contrast, it might be advantageous to judge the system from the liquidlike side of the transition. A phase transition to the solid phase may then be assigned when the liquid properties are lost. For that purpose, the method of instantaneous normal mode (INM) analysis provides an interesting description of the liquid behavior [17–21] especially for the case of supercooled liquids or liquids near freezing. For extended liquids, the INM analysis has been used to derive diffusion constants or solvation properties.

In this INM analysis, the frequencies of the instantaneous normal modes ω_α are obtained from the eigenvalues of the dynamical matrix at any instant of time, which are either real or imaginary. The resulting density of states

$$\rho(\omega) = \left\langle \sum \delta(\omega - \omega_\alpha) \right\rangle \tag{1}$$

is the averaged distribution of the normal mode frequencies with the normalization $\int d\omega \rho(\omega) = 1$. The total density of states can be split into the stable part $\rho_s(\omega)$ with real ω_α and the unstable part $\rho_u(\omega)$ with imaginary ω_α. In an instantaneous energy landscape of the liquid, real values of ω_α belong to potential wells in which the particles of the liquid can oscillate around their current equilibrium in the cage of the nearest neighbors. Imaginary values of ω_α represent the potential hills that separate the minima. Now, especially the unstable part $\rho_u(\omega)$ provides detailed information of the liquid behavior since the the thermal energy drives configurational transitions to take place over these potential hills. The unstable part of the density of states is closely related to liquid properties, such as the diffusion constant D. This can be understood because the crossing over the potential barriers characterizes the transient behavior of the liquid.

In this Letter, we will determine the phase transitions of a large number of charged-particle clusters in a dusty plasma, which are thermodynamically heated by lasers. We adapt the INM analysis to finite dust clusters to derive liquid transport constants, such as the diffusion constant. From the diffusion constants, the solid-liquid phase transition is approached from the liquid side, and freezing temperatures are derived and compared to the stability properties of the cluster arrangements.

The experiments have been performed in a dusty plasma where plastic microspheres are trapped in a gaseous discharge plasma (see Refs. [5,6,8,22,23]). The plasma was ignited in argon at a gas pressure of 7 Pa using a radio-frequency discharge ($f_{\mathrm{RF}} = 13.56$ MHz) at a power of

3 W. In this plasma, a small number N of microspheres was trapped to form two-dimensional finite dust clusters. The microspheres were 12.26 μm melamine-formaldehyde grains with a mass of $m = 1.5 \times 10^{-12}$ kg. The spheres attained a negative charge of $Z = 21\,900 \pm 2000$ elementary charges due to the continuous inflow of plasma electrons and ions. Vertically, the particles are trapped in a monolayer due to the strong confinement provided by gravity and electric fields in the space charge sheath. For horizontal confinement, the electrode has a very shallow spherical depression. The likewise curved equipotential planes trap the microspheres horizontally in a harmonic confinement of trap frequency $\omega_0 = 6.4 \pm 1.0\ \mathrm{s}^{-1}$. The particle motion is recorded with high-resolution CCD cameras at a frame rate of 60 frames/s which is decisively faster than the typical plasma (Debye) frequency of the cluster $\omega_{\mathrm{pd}} = (Z^2e^2/(\pi\epsilon_0 m b^3))^{1/2} = 15\ \mathrm{s}^{-1}$ with the elementary charge e, the dielectric constant ϵ_0, and the interparticle distance $b = 1.1$ mm.

The dust clusters are heated by an in-plane four-axis laser system [24] where the laser beams randomly "kick" the microspheres on both horizontal axes in both directions by radiation pressure forces. The random process of laser "kicks" is chosen in such a way that the kinetic energies of the microspheres are isotropic with a nearly Maxwellian velocity distribution. Hence, the particles gain a temperature T in a true thermodynamic sense [24].

The experiments shown here have been performed on dust clusters with $N = 19$–50 particles. Here, 10–20 runs at different temperatures have been realized for each cluster. Each run covers an observation time of 250 s (corresponding to 15 000 frames), which is long enough to allow for a large number of slow configurational changes in the liquid phase. As an example, Fig. 1 shows the trajectories of the particles in the $N = 19$ dust cluster for three different heating temperatures. Together with the trajectories, the INM density of states ρ is shown for these temperatures.

To calculate the INM, the instantaneous experimental positions of the particles in each frame have been used. For the dynamical matrix the particles are, as in the experiment, assumed to be trapped in a harmonic 2D confinement potential and to interact via a shielded Yukawa (Debye) potential. The dynamical matrix is fully determined by a single experiment parameter: the screening strength $\kappa = r_0/\lambda_{\mathrm{D}}$ defined as the spatial scaling $r_0 = (2Z^2e^2/(4\pi\epsilon_0 m\omega_0^2))^{1/3}$ in units of the shielding (Debye) length λ_{D} [15]. Here, a fixed value of $\kappa = 1$ has been used as determined from previous experiments [7,23]. The $2N$ eigenfrequencies (either real or imaginary) in all the 15 000 frames then constitute the density of states ρ.

It is seen from the trajectories that the cluster develops from an unordered arrangement ("liquid state") at the high temperature, where frequent intershell transitions occur, to an ordered arrangement ("solid state") at low temperature. At the medium temperature the excursions of the innershell particles start to overlap, indicating the onset of loss of angular order, and a few intershell transitions are recognized.

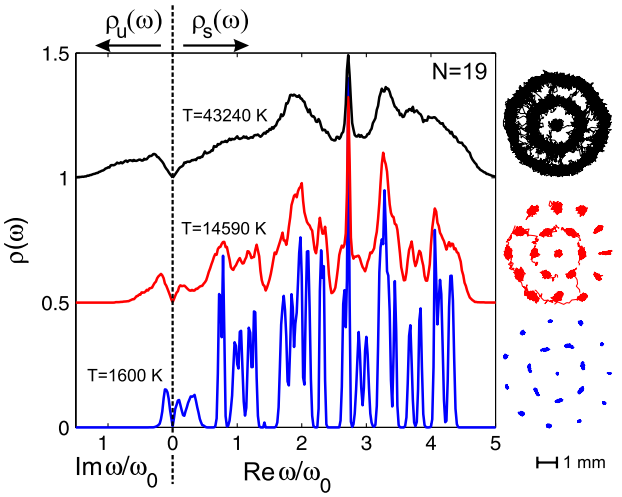

FIG. 1 (color online). Density of states ρ of the dust cluster with $N = 19$ at three different temperatures achieved by laser heating. The different curves are vertically shifted by 0.5 for clarity. As usual, the unstable part $\rho_u(\omega)$ with the imaginary eigenfrequencies is plotted as $\rho_u(|\omega|)$ on the negative frequency axis. Corresponding trajectories of the cluster particles over 250 s are also shown.

The density of states reflects this behavior. For the lowest temperature, ρ shows a very peaked structure, indicating that only certain modes at specific frequencies can occur in this ordered state. This state density very much resembles that found for the solid ground state [25,26] except for the small unstable part. For higher temperatures, a more continuous mode spectrum $\rho(\omega)$ is found, reflecting the disordered arrangement. As mentioned above, especially the unstable part of the state density ρ_u reflects the liquid behavior. The unstable part (plotted here, as usual, on the negative frequency axis) becomes much broader with increasing temperature. Also, the fraction of unstable modes compared to the total density increases from about 2% at $T = 1600$ K to about 8% at $T = 43\,240$ K. These findings already qualitatively demonstrate the change from a solidlike to a liquidlike cluster.

Now, to quantitatively address the liquid state of these clusters, liquid transport properties are determined from the INM modes. As the most important transport coefficient in a liquid, the diffusion constant D is presented here. The diffusion constant is derived from the relation [18,20]

$$D = \frac{k_{\mathrm{B}}T}{m} \int d\omega \rho(\omega) \frac{\tau_h}{1 + \tau_h^2\omega^2}, \qquad (2)$$

where τ_h is the average waiting time that is associated with the transition across potential barriers to other local minima in the momentary many-body potential surface of the

liquid (see also [27]). Following the method of Vijayadamodar and Nitzan [20], the corresponding hopping frequency τ_h^{-1} is given by

$$\tau_h^{-1} = c \int d\omega \rho(\omega) \frac{\omega}{2\pi} A \exp\left(-B\frac{\omega^2}{kT}\right), \qquad (3)$$

where $c \approx 3$ is associated with the different possibilities of escape routes from a potential minimum [28]. The parameters A and B are obtained, with an error of about 2%, from fitting $\rho_u(|\omega|)/\rho_s(\omega)$ to the function $A\exp(-B\omega^2/kT)$. As shown in the inset of Fig. 2, this functional form very well fits the behavior of $\rho_u(|\omega|)/\rho_s(\omega)$ from the experiment at all temperatures except the very lowest, where we expect the cluster to be in the solid state. These fits are given for the $N = 19$ cluster close to the freezing point ($T = 6700$ K) and in the liquid regime ($T = 14\,590$ K and 43 240 K, respectively).

The so-determined diffusion constants are shown in Fig. 2 for the 19- and 20-particle cluster as a function of cluster temperature. It is seen that the diffusion constant increases roughly linearly for both clusters above a threshold temperature. The diffusion constant takes values up to $D = 6 \times 10^{-9}$ m^2/s. For extended 2D systems under similar conditions, values in the range $D = 10^{-9}$–10^{-7} m^2/s [29–31] were reported. These values are in the range of those we find here for our finite systems, and especially the diffusion constants given by Vaulina *et al.* [29] match our results very well.

It is seen that the same magnitude of the diffusion constant is reached for the 19-particle clusters at higher temperatures. This reflects the higher stability of this cluster compared to the 20-particle cluster. The 19-particle cluster has a ground state configuration (1,6,12) with 1 particle in the center, 6 in the inner ring, and 12 in the outer. This is a "magic number" configuration due to the commensurate number of particles in the inner and outer ring with a high structural and dynamical stability. In the experiment, at the very low temperatures the 19-particle cluster happened to be in a metastable (1,7,11) configuration that has a low structural and dynamical stability due to the incommensurate particle numbers. However, upon laser heating the cluster "snapped" back into the more stable (1,6,12) configuration (see structures in Fig. 1). The 20-particle cluster has throughout a (1,7,12) configuration with incommensurate particle numbers and, hence, very low stability [6,23,25].

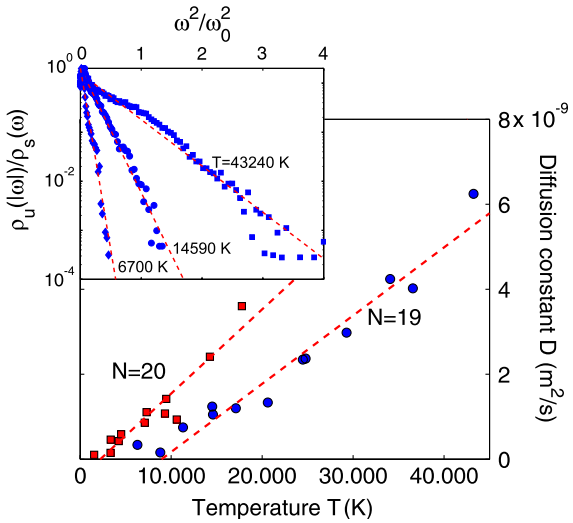

FIG. 2 (color online). Diffusion constant D as a function of cluster temperature for both the $N = 19$ (circles) and $N = 20$ (squares) particle clusters calculated from INM. The symbol size approximately corresponds to the errors in D (for fixed c). The dashed lines indicate a linear fit to the INM data to determine the melting temperature. The inset shows the ratio $\rho_u(|\omega|)/\rho_s(\omega)$ as a function of ω^2 for $N = 19$ together with the best exponential fit.

It should be noted that the hopping frequencies determined in this calculation are of the order of $\tau_h^{-1} = 0.1$ Hz for $N = 19$ and $\tau_h^{-1} = 1.5$ Hz for $N = 20$ at the highest temperatures. This is of the order of the frequency of intershell transitions seen in the trajectories (compare Fig. 1).

It is now very tempting to extrapolate the diffusion constants acquired by INM to $D \to 0$ to identify the freezing point, thereby assuming that in the solid regime the diffusion constant is much smaller than in the liquid. Hence, the freezing transition temperature is approached from the liquid phase of the cluster, here. In doing so [32], we find $T_M = 1650 \pm 550$ K for $N = 20$ and $T_M = 6700 \pm 2200$ K for $N = 19$, again reflecting the higher stability of the 19-particle cluster.

The so-determined melting temperature lies, for the $N = 19$ cluster, in a range where quite noticeable angular excursions of the particles are seen but where no angular transitions occur yet (compare Fig. 1). For the $N = 20$ cluster the melting temperature is found where angular transitions just have started to occur. Hence, the INM analysis of the liquid properties of finite charged-particle clusters seems to relate the solid-liquid phase transition to the loss of angular order of these clusters.

We have repeated these heating experiments and the INM analysis for a large number of clusters with different particle numbers between $N = 19$ and $N = 50$. In each case the diffusion constants as a function of temperature are determined, and then the melting temperatures are derived by extrapolating to $D \to 0$. The so-determined melting temperatures are shown in Fig. 3. It is seen that the melting temperature decisively depends on the exact particle number. A big variation of melting temperature is seen for the most prominent pair of $N = 19$ and 20, as discussed above. Relatively high melting temperatures are found for $N = 22$, 25, and 29 and relatively low temperatures for $N = 21$, 23, and 26. The Coulomb coupling parameter at melting $\Gamma_M = Z^2e^2/(4\pi\epsilon_0 b k_B T_M)$ ranges from $\Gamma_M = 900$ (for $N = 21$) to $\Gamma_M = 5500$ (for $N = 19$). Values in this range might be expected

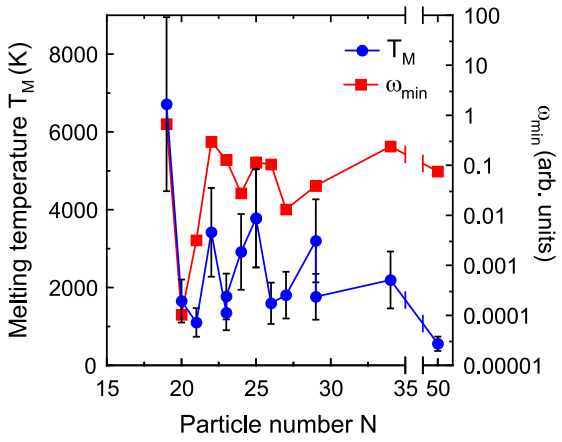

FIG. 3 (color online). Melting temperature (circles) as a function of cluster size, i.e., particle number N. For comparison, the frequency of the lowest frequency mode is shown (squares, data from [25]).

when taking into account finite size effects [9] and screening [33].

The assignment of a single freezing temperature certainly is to be taken with care since the melting usually is a two-step process (angular and radial melting) and might also differ between the different shells of the cluster [10,25]. Hence, to judge the quality of the above-described freezing temperature, we compare with stability criteria obtained from simulations in Ref. [25]. These authors have shown that the mode with the lowest eigenfrequency determines the stability of the cluster. For small clusters, this lowest-frequency mode usually corresponds to intershell rotation, for larger to vortex-antivortex motion. Here, the frequency of the lowest-frequency mode ω_{min} is given in comparison to the melting temperatures in Fig. 3.

It is seen that the melting temperature derived from the INM diffusion constants qualitatively matches the behavior of the minimum excitation frequency ω_{min}. The high freezing temperature of the $N = 19$ cluster goes along with a high excitation frequency and, hence, a high stability against perturbations. In the same way, the $N = 20$ system has a low freezing temperature and a low excitation frequency. Our freezing temperatures obtained from INM correlate well with the minimum excitation frequency for all particle numbers. For larger clusters, $N = 34$ and 50; however, the correspondence is not as close as for the smaller clusters. This is due to the fact that the configuration realized in the experiment does not correspond to the ground-state configuration of the simulation with pure Coulomb interaction. Consequently, also the minimum excitation frequency from the simulation will not exactly correspond to the experimental situation. Nevertheless, the freezing temperatures determined here are very well related to the minimum excitation frequencies.

In conclusion, our controlled laser-heating experiments together with the described analysis opens up new possibilities to study the fluid properties of charged-particle clusters in terms of reliable diffusion constants, hopping rates, and melting temperatures. These now allow us to address the solid-fluid phase transition from the fluid state and to determine the point where the liquid properties are lost. This is complementary to the usual approach where one is interested in identifying the loss of order. Another advantage of INM lies in the fact that all $2N$ eigenfrequencies ω_α in each time step enter the analysis whereas in other methods, e.g., using distance fluctuations [16], only a single parameter is calculated from the configuration in each time step, thus requiring a much longer time series for the same statistics. Hence, this method is capable to determine the stability of finite clusters from experiments, allowing us to reveal detailed insight into the phase transition behavior of finite systems and to characterize fluid finite systems.

We gratefully acknowledge financial support from DFG under Grant No. SFB-TR24, Projects A2 and A3.

[1] A. Proykova and R. S. Berry, J. Phys. B **39**, R167 (2006).
[2] A. Mortensen, E. Nielsen, T. Matthey, and M. Drewsen, Phys. Rev. Lett. **96**, 103001 (2006).
[3] P. Leiderer, W. Ebner, and V. B. Shikin, Surf. Sci. **113**, 405 (1982).
[4] A. V. Filinov, M. Bonitz, and Y. Lozovik, Contrib. Plasma Phys. **41**, 357 (2001).
[5] W.-T. Juan, Z.-H. Huang, J.-W. Hsu, Y.-J. Lai, and L. I, Phys. Rev. E **58**, R6947 (1998).
[6] M. Klindworth, A. Melzer, A. Piel, and V. A. Schweigert, Phys. Rev. B **61**, 8404 (2000).
[7] A. Melzer, M. Klindworth, and A. Piel, Phys. Rev. Lett. **87**, 115002 (2001).
[8] F. M. H. Cheung, C. Brunner, A. A. Samarian, and B. W. James, AIP Conf. Proc. **799**, 185 (2005).
[9] J. P. Schiffer, Phys. Rev. Lett. **88**, 205003 (2002).
[10] V. M. Bedanov and F. M. Peeters, Phys. Rev. B **49**, 2667 (1994).
[11] Y. Lozovik and E. Rakoch, Phys. Lett. A **240**, 311 (1998).
[12] G. Astrakharchik, A. Belousov, and Y. Lozovik, JETP **89**, 696 (1999).
[13] A. V. Filinov, M. Bonitz, and Y. E. Lozovik, Phys. Rev. Lett. **86**, 3851 (2001).
[14] H. Totsuji, Phys. Plasmas **8**, 1856 (2001).
[15] M. Kong, B. Partoens, and F. M. Peeters, New J. Phys. **5**, 23 (2003).
[16] J. Böning, A. Filinov, P. Ludwig, H. Baumgartner, M. Bonitz, and Y. E. Lozovik, Phys. Rev. Lett. **100**, 113401 (2008).
[17] G. Seeley and T. Keyes, J. Chem. Phys. **91**, 5581 (1989).
[18] T. Keyes, J. Phys. Chem. A **101**, 2921 (1997).
[19] R. M. Stratt, Acc. Chem. Res. **28**, 201 (1995).
[20] G. V. Vijayadamodar and A. Nitzan, J. Chem. Phys. **103**, 2169 (1995).

[21] J. D. Gezelter, E. Rabani, and B. J. Berne, J. Chem. Phys. **107**, 4618 (1997).
[22] H. Thomas, G. E. Morfill, V. Demmel, J. Goree, B. Feuerbacher, and D. Möhlmann, Phys. Rev. Lett. **73**, 652 (1994).
[23] A. Melzer, Phys. Rev. E **67**, 016411 (2003).
[24] J. Schablinski, D. Block, A. Piel, A. Melzer, H. Thomsen, H. Kählert, and M. Bonitz, Phys. Plasmas **19**, 013705 (2012).
[25] V. A. Schweigert and F. M. Peeters, Phys. Rev. B **51**, 7700 (1995).
[26] K. Nelissen, A. Matulis, B. Partoens, M. Kong, and F. M. Peeters, Phys. Rev. E **73**, 016607 (2006).
[27] Z. Donkó, G. J. Kalman, and K. I. Golden, Phys. Rev. Lett. **88**, 225001 (2002).
[28] By changing c between 1 and 10 the absolute values of the diffusion constants change by a factor of about 5, but the $D(T)$ characteristic remains unchanged.
[29] O. Vaulina and S. V. Vladimirov, Phys. Plasmas **9**, 835 (2002).
[30] B. Liu and J. Goree, Phys. Rev. Lett. **100**, 055003 (2008).
[31] L.-J. Hou, A. Piel, and P. K. Shukla, Phys. Rev. Lett. **102**, 085002 (2009).
[32] The error range of the freezing temperature accounts for the variation of the screening strength in the range $\kappa = 0$–3 [7,23] and the parameter c in Eq. (3) in the range $c = 1$–10 [20].
[33] S. Hamaguchi, R. T. Farouki, and D. H. E. Dubin, Phys. Rev. E **56**, 4671 (1997).